Supplemental information for

Depth of diamond formation obtained from single periclase inclusions

Chiara Anzolini[1*], Fabrizio Nestola[1], Mattia L. Mazzucchelli[2], Matteo Alvaro[2], Paolo Nimis[1], Andrea Gianese[1], Simone Morganti[3], Federica Marone[4], Marcello Campione[5], Mark T. Hutchison[6], and Jeffrey W. Harris[7]

[1]*Department of Geosciences, University of Padova, Via G. Gradenigo 6, 35131 Padova, Italy (chiara.anzolini@phd.unipd.it, fabrizio.nestola@unipd.it, paolo.nimis@unipd.it, andrea.gianese.1@studenti.unipd.it)*

[2]*Department of Earth and Environmental Sciences, University of Pavia, Via A. Ferrata 1, 27100 Pavia, Italy (mattialuca.mazzucchelli01@universitadipavia.it, matteo.alvaro@unipv.it)*

[3]*Department of Electrical, Computer, and Biomedical Engineering, University of Pavia, Via A. Ferrata 5, 27100 Pavia, Italy (simone.morganti@unipv.it)*

[4]*Swiss Light Source, Paul Scherrer Institut, 5232 Villigen, Switzerland (federica.marone@psi.ch)*

[5]*Department of Earth and Environmental Sciences, University of Milano Bicocca, Piazza della Scienza 4, 20126 Milan, Italy (marcello.campione@unimib.it)*

[6]*Trigon GeoServices Ltd., 2780 South Jones Blvd, Ste 35-15, Las Vegas, NV 89146, USA (mth@trigon-gs.com)*

[7]*School of Geographical and Earth Sciences, University of Glasgow, G12 8QQ Glasgow, UK (Jeff.Harris@glasgow.ac.uk)*

*Current address: Department of Earth and Atmospheric Sciences, 1-26 Earth Sciences Building, University of Alberta, Edmonton, Alberta T6G 2E3, Canada; E-mail: chiara.anzolini@phd.unipd.it.

Finite Element (FE) Analysis

The FE analysis was performed on the real 3-D model built from the segmentation of the X-ray microtomographic data (Fig. 2). The surface of the model was smoothed to improve the quality of the final FE mesh, having care not to obliterate the surface topography of the inclusions. The final 3-D model was then assembled placing the two inclusions in the diamond host. An elastically isotropic analysis was run with Simulia Abaqus, a commercial engineering package for FE analysis (http://abaqus.software.polimi.it/v2016/; for more details on the procedure see Mazzucchelli et al., 2018). The elastic properties for the ferropericlase (fper) inclusions were obtained fitting the original pressure-volume-temperature P-V-T data of Mao et al. (2011) up to 2000 K and 50 GPa using a 3rd-order Birch-Murnaghan Equation of State (EoS) combined with a Berman-type thermal expansion, that gives an isothermal bulk modulus K_{0TR} = 162(14) GPa (full EoS reported at http://www.rossangel.com). The Reuss shear modulus G_{0R} = 87(2) GPa was obtained from the elastic constants reported by Jacobsen et al. (2002) for a fper with composition $(Mg_{0.63}Fe_{0.37})O$ that is close to the composition of our inclusions, $(Mg_{0.60}Fe_{0.40})O$. For diamond we used the K_{0TR} = 444(2) GPa from the P-V-T EoS reported by Angel et al. (2015a) and the G_{0TR} = 535 GPa reported by Angel et al. (2015b).

Elastoplastic Model

The calculation is split into two steps dividing the calculation into an isothermal, quasi-static decompression from entrapment conditions P_{trap}, T_{trap} to P_{room}, T_{trap}, followed by an isobaric cooling to room temperature. The model is solved by inversion. The host-inclusion system is initially at P_{room}, T_{room} with the inclusion at the experimentally measured P_{inc}^{exp}. First, an entrapment temperature (T_{trap}) is chosen and the over-pressure $P_{inc}^{P_{room}, T_{trap}}$ developed in the inclusion during isobaric heating to P_{room}, T_{trap} is calculated adjusting the elastic properties of the host and the inclusion according to their EoS. A P_{trap} is guessed at the chosen T_{trap}, and the elastoplastic deformation of the host and inclusion pressure are calculated during the quasi-static decompression

of the host from P_{trap}, T_{trap} to P_{room}, T_{trap} according to Campione (2018). The guessed P_{trap} is adjusted until the pressure calculated in the inclusion at P_{room}, T_{trap} matches the previously found $P_{inc}^{P_{room}, T_{trap}}$. The elastic properties for diamond are from Angel et al. (2015a) and from Zouboulis et al. (1998). The variation of σ_Y with T (between 1273 and 1823 K) was obtained from Weidner et al. (1994). The EoS of the inclusion was re-fitted from the data of Mao et al. (2011) as discussed above.

Magnesioferrite Exsolutions Within Ferropericlase Inclusions

Single crystal X-ray diffraction measurements on the two fper inclusions revealed the presence of another phase, which was identified as magnesioferrite. Diffraction images (Fig. DR2) only show the second (1.49 Å) and the third (2.44 Å) most intense peaks of fper, as the main peak (2.10 Å) cannot be detected due to an overlap with the most intense diamond peak, located at the same d spacing (2.07 Å). In addition, the first (2.53 Å) and the third (2.97 Å) most intense peaks of magnesioferrite are visible. Again, the second peak of magnesioferrite in order of intensity (1.48 Å) cannot be unambiguously detected due to overlapping with the peak of fper (1.49 Å). As indicated by the diffraction data, fper and the exsolutions of magnesioferrite show an almost identical crystallographic orientation. In order to produce pseudo-single-crystal X-ray diffraction spots like those shown in Fig. DR2, there must be a high density of nanometer-sized magnesioferrite grains in topotaxial relation to the fper, which was subsequently confirmed by FEG-SEM observations (Fig. DR1).

Figure DR1. Scanning Electron micrographs of a) inclusion AZ1_1; b) portion of inclusion AZ1_1; c) inclusion AZ1_2; d) portion of inclusion AZ1_2. The polished surface of both inclusions exhibits pervasively and homogeneously distributed nanometer-sized exsolutions of magnesioferrite, which represent ~6% of the total surface area (calculated using the ImageJ software, Abràmoff et al., 2004).
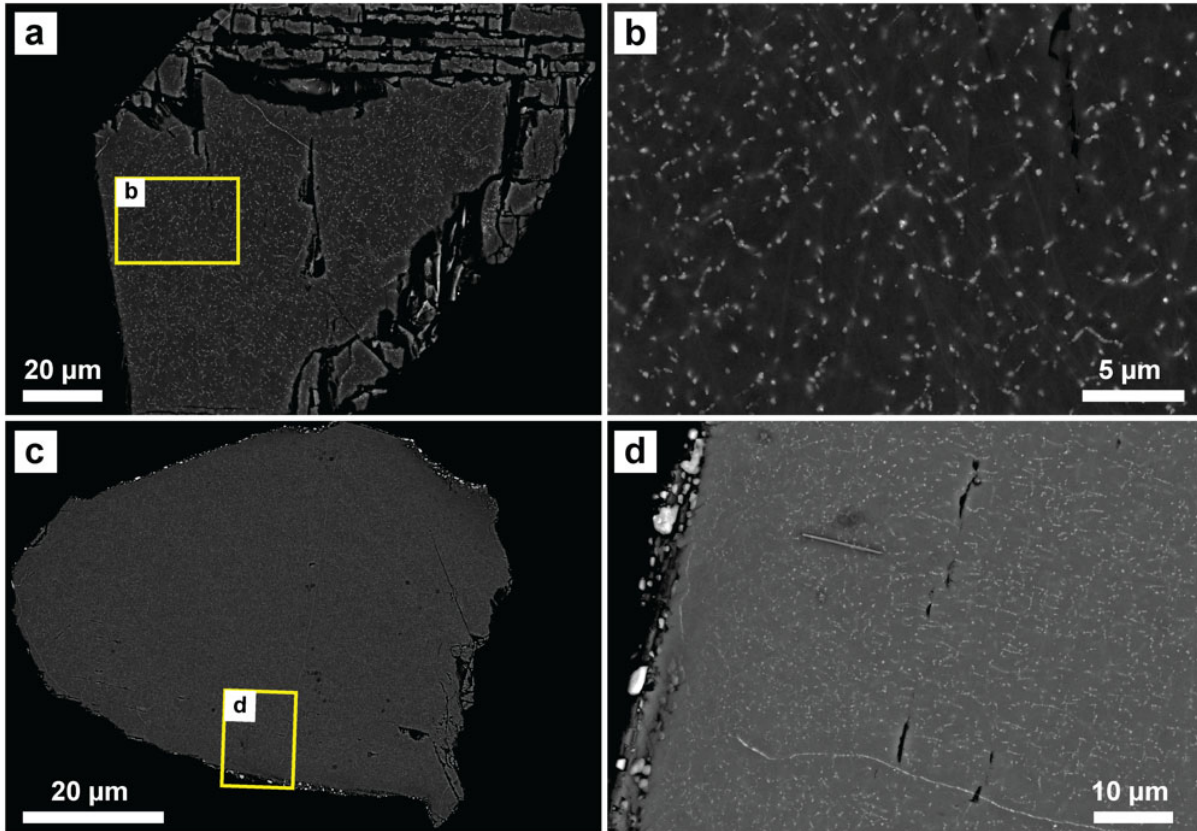
Figure DR2. Single-crystal X-ray diffraction images of inclusion AZ1_2 showing the second and the third diffraction peaks of ferropericlase together with the first and the third most intense peaks of magnesioferrite. Peaks at 2.07 Å and 1.26 Å belong to diamond.
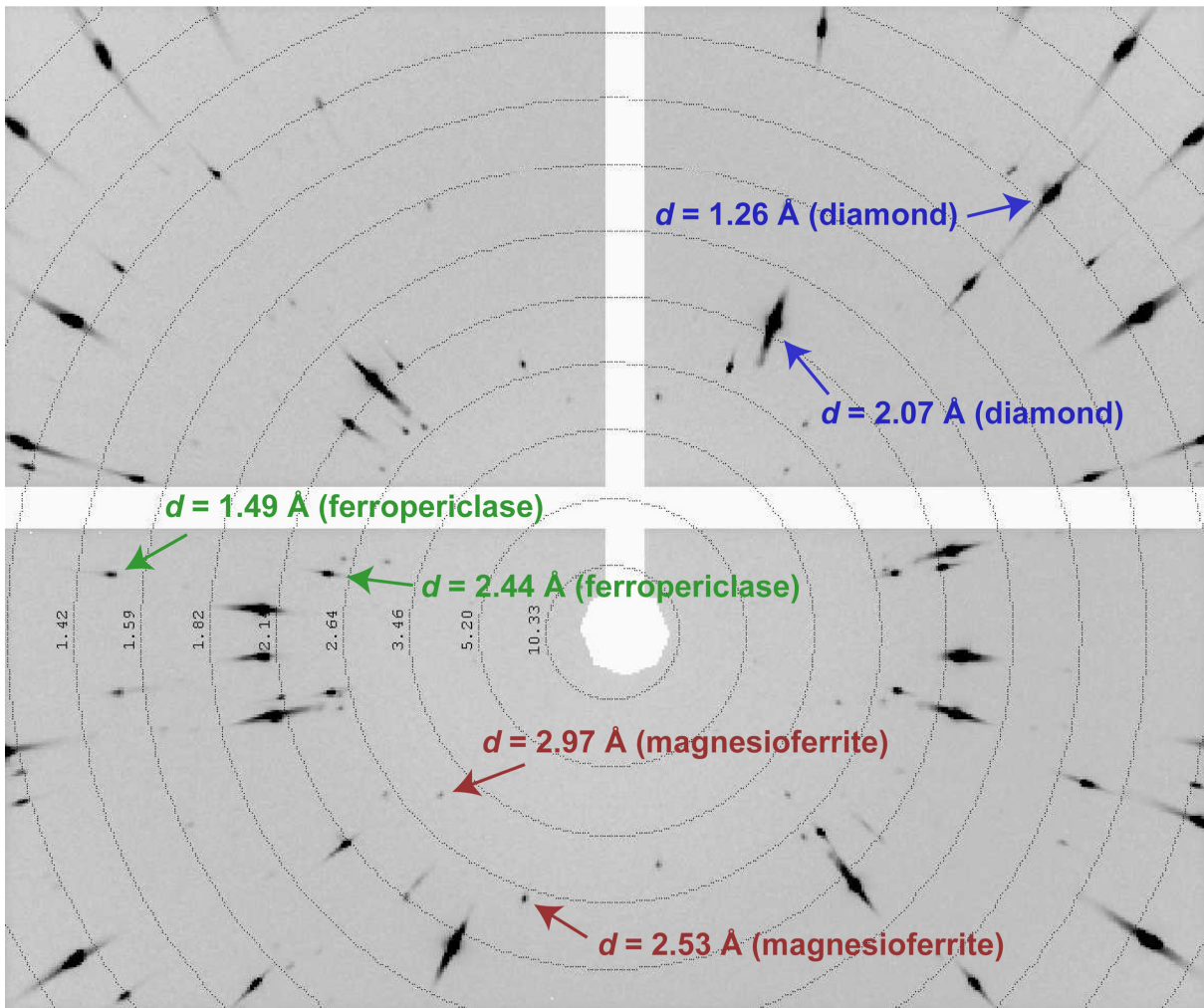
TABLE DR1. LATTICE PARAMETER AND UNIT-CELL VOLUME OF THE TWO FERROPERICLASE INCLUSIONS. THE RESIDUAL PRESSURE IS CALCULATED BY COMPARING THE VOLUME BEFORE (V) AND AFTER (V_0) RELEASE FROM THE DIAMOND HOST.

Inclusion	a (Å)	a_0 (Å)	V (Å^3)	V_0 (Å^3)	P_{inc} (GPa)
AZ1_1	4.253(4)	4.2685(2)	76.91(12)	77.770(5)	1.84(65)
AZ1_2	4.256(8)	4.2689(3)	77.1(2)	77.795(9)	1.48(67)

TABLE DR2. ISOMEKE CALCULATIONS FOR THE TWO DIAMOND-FERROPERICLASE HOST-INCLUSION SYSTEMS STUDIED IN THIS WORK.

T (K)	P_{trap} inclusion AZ1_1			P_{trap} inclusion AZ1_2		
	P_{inc} − esd	P_{inc} = 1.87	P_{inc} + esd	P_{inc} − esd	P_{inc} = 1.61	P_{inc} + esd
1448	10.26	11.74	13.25	09.54	11.15	12.81
1498	10.52	11.99	13.51	09.80	11.41	13.07
1548	10.77	12.25	13.76	10.05	11.66	13.32
1598	11.02	12.49	14.01	10.29	11.90	13.57
1648	11.26	12.73	14.25	10.53	12.14	13.81
1698	11.49	12.97	14.48	10.77	12.38	14.04
1748	11.72	13.20	14.71	11.00	12.61	14.27
1798	11.95	13.42	14.94	11.22	12.83	14.50
1848	12.16	13.64	15.16	11.44	13.05	14.72
1898	12.38	13.85	15.37	11.66	13.27	14.93
1948	12.59	14.06	15.58	11.87	13.48	15.14
1998	12.79	14.27	15.78	12.07	13.68	15.34

Note: P_{trap} and P_{inc} are expressed in GPa.

REFERENCES CITED

Abaqus, 2016, Abaqus Documentation: Providence, Rhode Island, Dassault Systèmes, http://50.16.225.63/v2016/.

Abràmoff, M.D., Magalhães, P.J., and Ram, S.J., 2004, Image processing with ImageJ: Biophotonics International, v. 11, p. 36–42.

Angel, R.J., Alvaro, M., Nestola, F., and Mazzucchelli, M.L., 2015a, Diamond thermoelastic properties and implications for determining the pressure of formation of diamond-inclusion systems: Russian Geology and Geophysics, v. 56, p. 211–220, https://doi.org/10.1016/j.rgg.2015.01.014.

Angel, R.J., Nimis, P., Mazzucchelli, M.L., Alvaro, M., and Nestola, F., 2015b, How large are departures from lithostatic pressure? Constraints from host–inclusion elasticity: Journal of Metamorphic Geology, v. 33, p. 801–813, https://doi.org/10.1111/jmg.12138.

Campione, M., 2018, Threshold effects for the decrepitation and stretching of fluid inclusions: Journal of Geophysical Research: Solid Earth, v. 123, p. 3539–3548, https://doi.org/10.1029/2018JB015694.

Jacobsen, S.D., Reichmann, H.J., Spetzler, H.A., Mackwell, S.J., Smyth, J.R., Angel, R.J., and McCammon, C.A., 2002, Structure and elasticity of single-crystal (Mg,Fe)O and a new method of generating shear waves for gigahertz ultrasonic interferometry: Journal of Geophysical Research Solid Earth, v. 107, ECV 4–1–ECV 4–14, https://doi.org/10.1029/2001JB000490.

Mao, Z., Lin, J., Liu, J., and Prakapenka, V.B., 2011, Thermal equation of state of lower-mantle ferropericlase across the spin crossover: Geophysical Research Letters, v. 38, L23308, https://doi.org/10.1029/2011GL049915.

Mazzucchelli, M.L., Burnley, P., Angel, R.J., Morganti, S., Domeneghetti, M.C., Nestola, F., and Alvaro, M., 2018, Elastic geothermobarometry: Corrections for the geometry of the host-inclusion system: Geology, v. 46, p. 231–234, https://doi.org/10.1130/G39807.1.

Weidner, D.J., Wang, Y., and Vaughan, M.T., 1994, Strength of diamond: Science, v. 266, p. 419–422, https://doi.org/10.1126/science.266.5184.419.

Zouboulis, E.S., Grimsditch, M., Ramdas, A.K., and Rodriguez, S., 1998, Temperature dependence of the elastic moduli of diamond: A Brillouin-scattering study: Physical Review B: Condensed Matter and Materials Physics, v. 57, p. 2889–2896, https://doi.org/10.1103/PhysRevB.57.2889.